Ecologica Montenegrina
ISSN 2336-9744 (online) | ISSN 2337-0173 (print)

Ecologica Montenegrina 66: 120-143 (2023)
This journal is available online at: www.biotaxa.org/em
https://dx.doi.org/10.37828/em.2023.66.8

Article

Impact of aquatic habitat environment on the elemental composition and shell shape variability of the Beringian freshwater mussel *Beringiana beringiana* (Bivalvia, Unionidae)

ARTEM A. LYUBAS[1*], OLEG S. POKROVSKY[2,3], TATYANA A. ELISEEVA[1], ALEXANDER V. KONDAKOV[1], IRINA A. KUZNETSOVA[1], ILYA V. VIKHREV[1], EKATERINA S. KONOPLEVA[1], OLGA V. AKSENOVA[1], ALENA A. SOBOLEVA[1], MIKHAIL Y. GOFAROV[1], ALEXANDER V. KROPOTIN[1], MAXIM V. VINARSKI[4,5], ANDREY S. AKSENOV[6], ELENA V. LINNIK[7], IRINA S. KHREBTOVA[1], GALINA V. BOVYKINA[1] & IVAN N. BOLOTOV[1]

[1] *N. Laverov Federal Center for Integrated Arctic Research of the Ural Branch of the Russian Academy of Sciences, Nikolsky Av. 20, 163020 Arkhangelsk, Russia;*
https://orcid.org/0000-0001-7214-9822; https://orcid.org/0000-0002-6305-6496;
https://orcid.org/0000-0002-9530-0035; https://orcid.org/0000-0002-8612-7736;
https://orcid.org/0000-0002-4820-4921; https://orcid.org/0000-0002-0817-7105;
https://orcid.org/0000-0001-5550-5362; https://orcid.org/0000-0002-8532-0307;
https://orcid.org/0000-0002-9830-5472; https://orcid.org/0000-0002-1758-647X;
https://orcid.org/0000-0002-6723-3277; https://orcid.org/0000-0002-3878-4192
[2] *Geosciences and Environment Toulouse, UMR 5563 CNRS, 31400 Toulouse, France;*
https://orcid.org/0000-0002-3155-7069
[3] *BIO-GEO-CLIM Laboratory, Tomsk State University, 634050 Tomsk, Russia.*
[4] *Laboratory of Macroecology & Biogeography of Invertebrates, Saint Petersburg State University, Universitetskaya Emb. 7-9, 199034 Saint Petersburg, Russia; https://orcid.org/0000-0002-7644-4164*
[5] *Laboratory of Systematics and Ecology of Invertebrates, Omsk State Pedagogical University, Tukhachevskogo Emb. 14, 644099, Omsk, Russia.*
[6] *Northern (Arctic) Federal University, Northern Dvina Emb. 17, 163002 Arkhangelsk, Russia;*
https://orcid.org/0000-0003-1013-1357
[7] *Kurilsky Nature Reserve, Zarechnaya 5, 694500 Yuzhno-Kurilsk, Russia.*
* *Corresponding author: E-mail: lyubas@ro.ru; https://orcid.org/0000-0002-0558-0783*

Received 18 November 2023 | Accepted by *V. Pešić*: 22 December 2023 | Published online 26 December 2023.

Abstract
Concentrations of the chemical elements were analyzed in the shells of a bivalve mollusk species (*Beringiana beringiana*), water, and bottom sediments from seven lakes located on the Kamchatka Peninsula, the Kurile Islands, Sakhalin Island, and Primorsky Krai (Northeast Asia). A principal component analysis allowed to determine three factors those were related to environments in the waterbodies. We revealed two groups of samples corresponding to large geographical regions using the determined factors. Statistically significant differences were found between geographical groups of samples, and higher values of element distribution coefficients were determined for samples from lakes on the Kamchatka Peninsula. The highest concentrations of lithophilic elements were measured in the shells

from Lake Kurazhechnoye (Kamchatka Peninsula). The highest concentrations of Al and Mg were detected in shells from Lake Peschanoye (Kunashir Island). In Lake Chernoye (Sakhalin Island), the highest concentrations of Sr and Sb in the shells were detected. Zn, Fe, Pb, and rare earth elements were present in large concentrations in the shells from Lake Vaskovskoye, Primorsky Krai. The shells of the Beringian freshwater mussel show large phenotypic plasticity, and their shape demonstrates significant relationships with various environmental parameters, that were assessed based on the geochemical indicators.

Key words: freshwater mussels, *Beringiana beringiana,* trace elements, bioindicators, pollution, freshwater environment, Russian Far East, Northeast Asia.

Introduction

Freshwater bodies of Northeast Asia could be used as a source of useful information for evaluating environmental conditions that influence the biotic components of aquatic ecosystems. On the one hand, the territories of these geographic regions present pristine (intact) water basins on a wide scale, but on the other hand, there are local sources of water contamination that were assessed via chemical composition of waterbodies (e.g., lakes) and their invertebrate inhabitants (Chernova et al., 2014a; Golovaneva, 2016), including bivalve mollusks (Klishko et al., 2022). Trace elements in soft tissues of the Beringian freshwater mussel *Beringiana beringiana* (Middendorff, 1851) were described by Chernova et al. (2014b) in comparison with the water and bottom sediments from Primorsky Krai and Kamchatka regions. Moreover, these authors used soft tissues of freshwater mussels as an indicator of contamination of hydrobionts by heavy metals originated from industrial plants situated nearby (Chernova et al., 2014b; Bogatov & Bogatova, 2009; Bogatov et al., 2019). Thus, Bogatov et al. (2019) noted a relatively high concentration of lead in the soft tissues of *B. beringiana* (mentioned as *Kunashiria*) mussels from the Vaskovskoe Lake (Primorsky Krai). These authors related it to the influence of metallurgical plants via gaseous emissions, aerosol deposition, and industrial wastewater discharge from the lead smelter (Bogatov & Bogatova, 2009). Trace element composition of shells of *B. beringiana* mussels, and, also, water and bottom sediments from sites on the Kamchatka Peninsula (Khalaktyrskoe Lake) were accessed by Lyubas et al. (2023). Results of chemical studies of shells, water, and bottom sediment demonstrate a site-specific elemental composition of these materials.

Despite local sources of pollution, freshwater ecosystems of Northeast Asia provide a suitable environment for freshwater mussels from several ecological groups, varying from eurybiont species of the genera *Beringiana* and *Sinanodonta* to stenobiont species of the genus *Margaritifera*, inhabiting small watercourses in various freshwater basins in the region (Bolotov et al., 2015).

The chemical composition of freshwater pearl mussel shells (*Margaritifera* spp.) together with relevant environmental components were analyzed in the river basins of Kamchatka Peninsula, Sakhalin Island, and some islands of the Kuril Archipelago. The chemical composition of freshwater pearl mussel shells and water in several sites across Kamchatka and Kuril Islands showed patterns related to volcanic and hydrothermal activity in these regions (Bolotov et al., 2015). These authors demonstrated site-specific accumulation of trace elements among species of freshwater pearl mussels. However, the taxa of freshwater bivalves analyzed in Bolotov et al. (2015) mainly inhabit oligotrophic watercourses and hence do not provide representative data to assess environments in large freshwater basins in the studied region.

In the present study, we chose to work on the Beringian freshwater mussel (*B. beringiana)* for the following reasons. First, this species is widely distributed from Hokkaido Island in Japan and Primorsky Krai in Russia to Eastern Siberia and Kamchatka, as well as to the Aleutian Islands and the west coast of North America (Lopes-Lima et al., 2020). Therefore, these mussels may be used as the living bioindicator of environmental changes in freshwater ecosystems of the northeastern margin of Asia. Second, the Beringian freshwater mussel allows to analyze the influence of environmental changes on freshwater ecosystems within a wide gradient of habitats, from natural lakes to anthropogenically polluted water bodies. Third, *B. beringiana* is a conchologically variable species; a significant number of synonyms have been introduced for its morphotypes from different water bodies of the Russian Far East. The genus *Beringiana* is a distant phylogenetic lineage from the clade *Sinanodonta* belonging to the tribe Cristarini and is represented by a single species in the study area and several endemic species in Japan (Bolotov et al., 2020).

Therefore, one of the important tasks is verifying relationships between the shell shape and environmental conditions in waterbodies, assessed based on the chemical composition of abiotic components of the freshwater ecosystem in a certain habitat. Taken together, the use of *B. beringiana* as an indicator for assessing changes in environmental conditions in water bodies of the Far East seems to be a very urgent task.

The study aimed to (1) analyze major and trace element composition of *B. beringiana* shells and environmental compartments from several freshwater basins of the Russian Far East; (2) establish local patterns in the accumulation of major and trace elements by the Beringian freshwater mussel as indicator species; and (3) assess patterns of possible influence of local environmental conditions on the mussel shell shape.

Material and methods

Sampling

B. beringiana specimens were collected by hand from a depth of 0.5 to 2.0 m from seven sites across Northeast Asia in freshwater basins of the Kamchatka Peninsula (Khalaktyrka and Kamchatka River basins), Kurile Islands (Iturup and Kunashir islands), Sakhalin Island (Uglegorka River basin, Bolshoye Vavayskoye Lake) and Primorsky Krai (Vaskovskoye Lake) (Figure 1, Table 1).

Table 1. List of sampling localities.

№	Waterbody	Region	Number of analyzed specimens	Coordinates	
				Latitude	Longitude
1	Kurazhechnoye Lake	Kamchatka Peninsula	5	56.35995 N	160.88952 E
2	Khalaktyrskoye Lake	Kamchatka Peninsula	5	53.02736 N	158.73621 E
3	Lebedinoye Lake	Iturup Island	3	45.22933 N	147.91136 E
4	Peschanoye Lake	Kunashir Island	3	43.91929 N	145.63280 E
5	Chernoye Lake	Sakhalin Island	3	49.07523 N	142.10269 E
6	Bolshoye Vavayskoye Lake	Sakhalin Island	3	46.60463 N	143.19052 E
7	Vaskovskoye Lake	Primorsky Krai	3	44.34678 N	135.82299 E

The water was collected at the site of mollusks' sampling, by one sample from each site, from 0.5 m depth. A tissue snips from each specimen was preserved in 96% ethanol immediately after collection. The tissue snips and shells were deposited in the Russian Museum of Biodiversity Hotspots [RMBH], N. Laverov Federal Center for Integrated Arctic Research, the Ural Branch of the Russian Academy of Sciences, Arkhangelsk, Russia.

The water was immediately filtered through a single-use sterile acetate cellulose filter (Sartorius, 0.45 μm) into pre-cleaned polypropylene Nalgene bottles. Filtered water samples for major and trace element analyses were acidified with ultrapure double-distilled HNO_3 and stored in the refrigerator pending analyses. The sediment samples were taken from the water-sediment interface, by one sample from each site, encompassing 0–4 cm layer, which corresponded to the depth of burying of *B. beringiana* mussels in the bottom substrate. Samples were placed in sterile double-zip polyethylene bags, preserved in cold dark environment, and transported within several days to the laboratory where they were dried at 90 °C in the oven.

Species determination

For species identification, we analyzed the shell shape, and the sculpture and position of the umbo. Details of the shell structure were studied using Canon EOS 7D DSLR camera (Canon Inc., Japan). Collected specimens of freshwater mussels were compared with descriptions of freshwater bivalve species of the studied region published by Bolotov et al. (2020) and with the voucher specimens deposited in RMBH. The results of the morphological identification was verified based on nucleotide sequences of the specimens of bivalves using the Basic Local Alignment Search Tool, BLAST (Johnson et al., 2008).

Figure 1. Map of the studied region. Lakes: (1) Kurazhechnoye, Kamchatka Peninsula (*n* = 5), (2) Khalaktyrskoye, Kamchatka Peninsula (*n* = 5), (3) Lebedinoye, Iturup Island (n = 3), (4) Peschanoye, Kunashir Island (*n* = 3), (5) Chernoye, Sakhalin Island (*n* = 3), (6) Bolshoye Vavayskoye, Sakhalin Island (*n* = 3), (7) Vaskovskoye, Primorsky Krai (*n* = 3). *n* reveals the number of collected shells of *Beringiana beringiana*.

DNA extraction and sequencing

Total genomic DNA was extracted from available tissue snips using the NucleoSpin Tissue Kit (Macherey-Nagel GmbH and Co. KG, Germany), following the manufacturer's protocol. For molecular analyses, we obtained sequences of the mitochondrial *cytochrome c oxidase subunit I* (COI) gene fragment. The sequences were amplified and sequenced using primers LCO1490 and HCO2198 (Folmer et al., 1994). The PCR mix contained approximately 200 ng of total cellular DNA, 10 pmol of each primer, 200 μmol of each dNTP, 2.5 μl of PCR buffer (with 10 × 2 mmol $MgCl_2$), 0.8 units of Taq DNA polymerase (SibEnzyme Ltd., Russia), and H_2O, which was added up to a final volume of 25 μl. Thermocycling included one cycle at 95 °C (4 min), followed by 28–32 cycles of 95 °C (50 s), 46–48 °C (50 s), and 72 °C (50 s), and by a final extension at 72 °C (5 min). Forward and reverse sequencing was performed on an automatic sequencer (ABI PRISM3730, Applied Biosystems) using the ABI PRISM BigDye Terminator v.3.1 reagent kit. The resulting COI sequences were checked manually using BioEdit v. 7.2.5 (Hall, 1999).

Phylogeographic analysis

We used the COI dataset that included 50 sequences (total length of 612 bp) for the analysis (Appendix 1). The alignment of the COI sequences was performed directly using the ClustalW algorithm (Thompson et al., 1994). The phylogeographic analysis was carried out using a median-joining network approach with Network v. 5.0.0.1 software with default settings (Bandelt et al., 1999).

Analysis of shell shape (Fourier analysis)

The comparative analysis of the shell morphology was carried out with attention to the shell shape and umbo position. Shell shapes were analyzed using Fourier coefficients, which were calculated by software package SHAPE ver. 1.3 (Iwata & Ukai, 2002). Outlines of shells were obtained from photographs and digitized using GIMP v. 2.10. Prepared images in bitmap format were analyzed by ChainCoder program to describe geometric information about contours as a chain code in numbers from 0 to 7. Using Chc2Nef program we calculated the normalized Elliptic Fourier Descriptors (EFDs) based on the longest radius. The maximum number of harmonics was 20. During Chc2Nef processing all contours were orientated in the same position. Principal component analysis (PCA) was implemented on normalized EFD coefficients by PrinComp program. After that the shape variations explained by principal components (PCs) were visualized by drawing synthetic outlines of extreme (±2SD) shell shapes. Areas of each shell (mm^2) were calculated as the product of the area per pixel (mm^2) and the object area measured as the number of pixels. The scatter plot was created using PAST software (Hammer et al., 2001).

Determination of ontogenetic age of freshwater mussels

The ontogenetic age of mussel specimens was determined by counting of annual-ring number on the surface of the shell (Zotin & Popov, 2019).

Preparation of shells to chemical analyses

For the analysis of major and trace elements, parts of the shell were cut within the place of the maximal growth, from umbo towards the edges. We analyzed three to five mussel specimens from each locality. The samples were washed using MilliQ water, dried, and ground in an agate mortar followed by acid digestion in the clean room and ICP-MS analysis as described in details elsewhere (Bolotov et al., 2015; Lyubas et al., 2023).

Analysis of the major and trace element composition of shells, water, and bottom sediment samples

Mineralization of shell and sediment samples was carried out by acid digestion in Teflon Savillex vials. About 100 mg were used for analysis. Together with the analyzed samples, three blanks (without powder) and one certified standard material were digested. For control of the chemical yield during the sample decomposition procedure, to the aliquot of powder, we added 0.1 mL of a solution containing ^{145}Nd, ^{161}Dy, and ^{174}Yb (8 $\mu g/dm^3$), moistened with several drops of deionized water. Then, 0.5 mL of $HClO_4$ (Perchloric acid fuming 70% Supratur, Merck), 3 mL of HF (Hydrofluoric acid 40% GR, ISO, Merck), and 0.5 mL of HNO_3 (ultrapure, 65%, GR, ISO, Merck) were added and evaporated to intense white fumes, followed by cooling and washing from the vial walls. The residual solution was evaporated to wet salts. After that, 2 mL of HCl (ultrapure, fuming 37% GR, ISO, Merck) and 0.2 mL of 0.1 M H_3BO_3 solution (analytical grade) were added and the mixture was evaporated to a volume of 0.5–0.7 mL. The resulting solutions were transferred into pre-cleaned HDPE (high-density polyethylene) vials, into which 0.1 mL internal standard

(10 mg/L of In) was added and diluted with 2% HNO_3 to 20 mL (Karandashev et al., 2008). The concentrations of Li, Na, Mg, Al, P, S, K, Ca, Ti, Mn, Fe, Cu, Zn, Sr, Y, Zr, Sb, Ba, rare earth elements (REEs), and Pb were determined by ICP-MS (X-7, Thermo Scientific, Waltham, USA), which operated in He and no-gas mode. To control the accuracy of analyses of the mussel shells' elemental composition, in parallel with the samples, we processed two certified carbonate reference materials (Coral JCp-1, Giant Clam JCt-1).

Water samples were 0.45 μm filtered on-site and immediately acidified with concentrated ultrapure HNO_3 to 2%. The elemental composition of the water (Li, B, Na, Mg, Al, Si, P, S, K, Ca, Sc, Ti, V, Cr, Mn, Fe, Co, Ni, Cu, Zn, Ga, Ge, As, Se, Rb, Sr, Ba, Y, Zr, Nb, Mo, Cd, Sn, Sb, Cs, Ba, REE, Hf, W, Tl, Pb, Bi, Th, and U) was measured by ICP-AES. Certified reference materials of natural riverine water (SLRS-6) were used to monitor the accuracy of analyses.

Data treatment

Normality tests and comparisons were as follows. Prior to the computation, the data were converted to Ca-normalized concentrations, given that the aragonite ($CaCO_3$) matrix was the main component of the shells. Normality for each analyzed sample was determined based on Shapiro–Wilk's test significance values ($p > 0.05$). The Mann–Whitney U test was used to assess the differences in the concentrations in shell, water, and sediment samples between two samples. The Kruskal–Wallis H test was used for the measurement of the differences between the content of chemical elements in bivalve mollusk shells in several samples, and these data were ranked. Ranking consisted of the transition from the quantitative values of the concentrations of chemical elements to the ranks, which were subsequently compared with each other. Statistical analyses were carried out with use of PAST v 4.05.

Pairwise linear regression models were calculated in Microsoft Excel 2010 using the Analysis ToolPak. The significance of each model was estimated by F-test at $p < 0.05$.

Principal component analysis (PCA) was used to determine the factors controlling the pattern of element accumulation in shells, water, and sediments. The data from certain localities were classified according to revealed factors. The selection of factors was carried out according to the screen test and on the basis of eigenvalues (the Kaiser criterion). The suitability of the data for factorization was assessed based on the Kaiser–Meier–Olkin measure of sample adequacy (minimum fitness value was higher than 0.5) and using the Bartlett's test of sphericity ($p < 0.05$).

Results

Species determination

Conchologically, the collected specimens of freshwater mussels belonged to one species, the Beringian freshwater mussel *B. beringiana* (Figure 2). The average ontogenetic ages of studied individuals were 5.0 ± 0.0 years for Lake Chernoe ($n = 3$), 4.0 ± 0.0 years for Lake Peschanoye ($n = 3$), 3.7 ± 0.6 years for Lake Bolshoye Vavayskoye ($n = 3$), 4.0 ± 0.0 years for Lake Vaskovskoye ($n = 3$), 4.0 ± 0.0 years for Lake Lebedinoye ($n = 3$), 5.4 ± 0.6 years for Lake Kurazhechnoye ($n = 5$), 6.0 ± 0.0 years for Lake Khalaktyrskoye ($n = 5$).

Analyses of 24 COI gene sequences for collected mussels with length of 660 bp demonstrated that all mollusk specimens belong to *B. beringiana* that agrees with their conchological features. Totally, six unique COI haplotypes were identified in the studied sample from the Russian Far East.

Morphological patterns

Two significant principal components were obtained using PCA based on 20 EFDs. PC1 explained 52.1 % of total variation of sagittal shell shape, whereas PC2 explained 16.7 %. Six synthetic outlines of the extreme and mean shell forms are illustrated in Figure 3. The first component is responsible for changing the shape of the lower edge of the shell. The second component reflects the umbo position.

Phylogeographic and distributional patterns

Phylogeographic pattern demonstrated the presence of one widely distributed COI haplotype that was found across the entire range of the Beringian mussel in freshwater basins of Northeast Asia, Japanese Archipelago, and Alaska (Figure 4). Additionally, several COI haplotypes were recorded in distant waterbodies across the

abovementioned regions, mainly in Japan, Primorsky Krai, on the Kuril Islands, and in Alaska. These haplotypes have one to three nucleotide substitutions. Overall, the COI sequences of the Beringian freshwater mussel from large distribution area support the hypothesis of low genetic diversity of this species (Bulakhova et al., 2023).

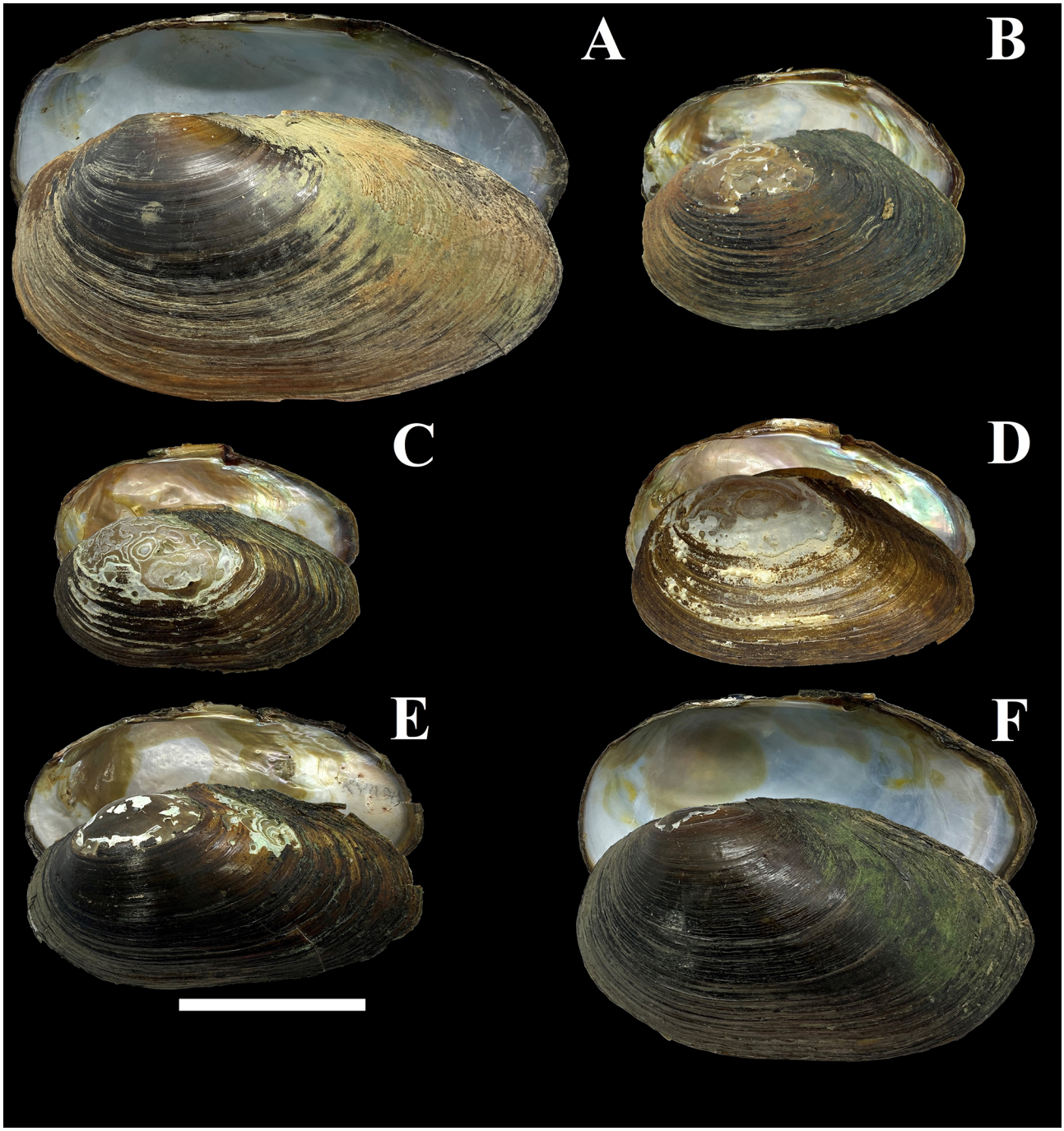

Figure 2. Shells of *Beringiana beringiana* specimens, collected from studied waterbodies: A – Kurazhechnoye Lake, Kamchatka Peninsula (voucher number RMBH biv1212/2), B – Vaskovskoye Lake, Primorsky Krai (RMBH biv1181/1), C – Lebedinoye Lake, Iturup Island (RMBH biv1254/2), D – Bolshoye Vavayskoye Lake, Sakhalin Island (RMBH biv1250/1), E - Peschanoye Lake, Kunashir Island (RMBH biv1251/1), F – Khalaktyrskoye Lake, Kamchatka Peninsula (RMBH biv1213/3). Scale bar = 50 mm.

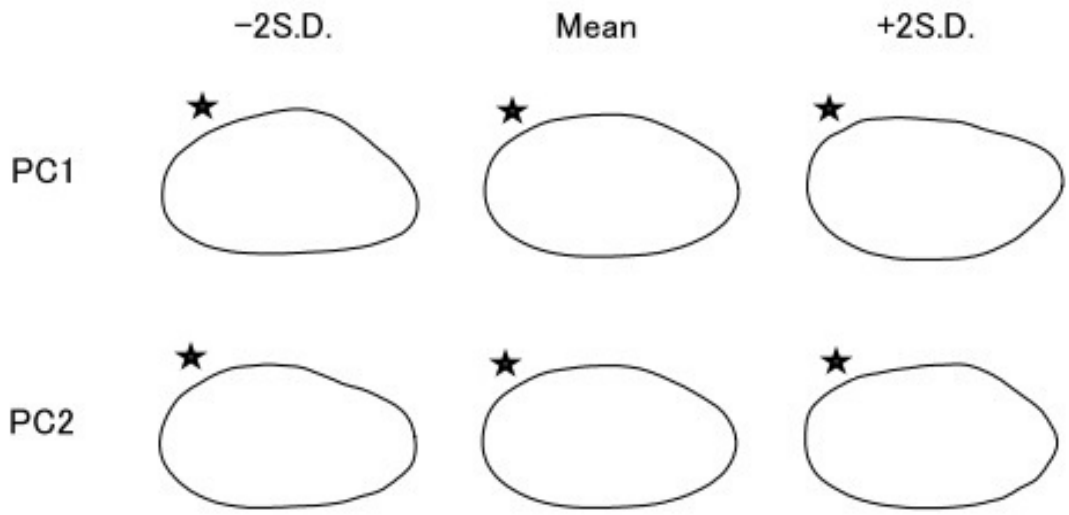

Figure 3. Principal components 1 and 2 visualized by drawing synthetic outlines of extreme (±2SD) and mean shell shapes of *Beringiana beringiana*. The umbo position marked by star.

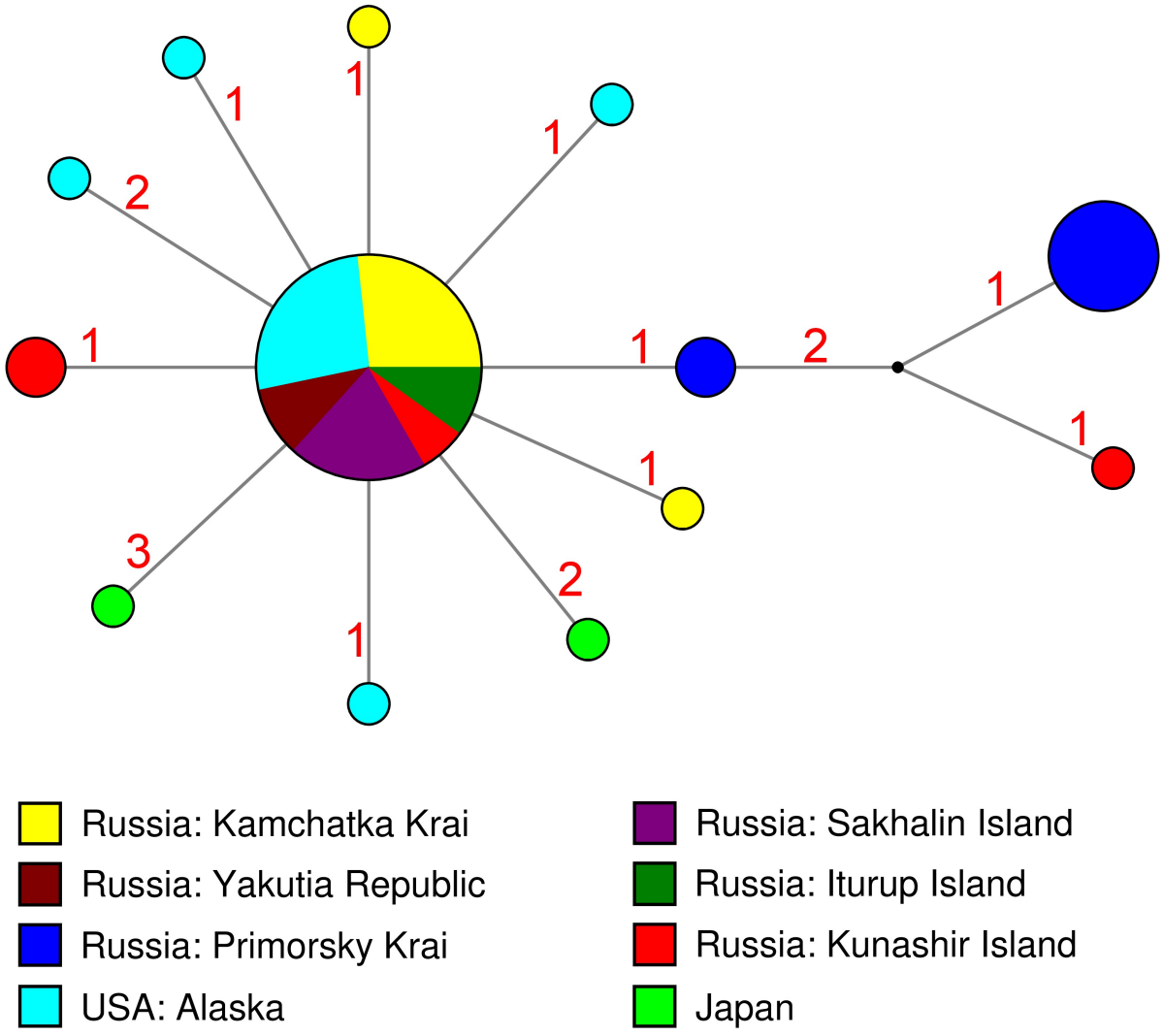

Figure 4. Median joining networks of *Beringiana beringiana* ($N = 50$) based on the COI gene fragment. The circle size is proportional to the number of available sequences belonging to the given haplotype (the smallest = 1 sequence). The red numbers near branches indicate the number of nucleotide substitutions between haplotypes.

Elemental composition of shells

The mean chemical composition of mollusk shells is presented in Table 2. After Ca, the most abundant elements were Na, Fe, Mn, Sr, S, Al, and Mg. Average concentrations of Na, Fe, Mn, Sr, S, Al, and Mg in *B. beringiana* shells (n = 25) were 1930±53 ppm, 789±156 ppm, 585±54 ppm, 520±51 ppm, 413±20 ppm, 136±24 ppm, and 81±11 ppm, respectively.

Table 2. Elemental composition of *Beringiana beringiana* shells (Mean ± SE, ppm) from the studied lakes.

Element	*Chernoye Lake, Sakhalin Island* (n = 3)	*Peschanoye Lake, Kunashir Island* (n = 3)	*Bolshoye Vavayskoye Lake, Sakhalin Island* (n = 3)	*Vaskovskoye Lake, Primorsky Krai* (n = 3)	*Lebedinoye Lake, Iturup Island* (n = 3)	*Kurazhechnoye Lake, Kamchatka Peninsula* (n = 5)	*Khalaktyrskoye Lake, Kamchatka Peninsula* (n = 5)
Li	0.088±0.026	0.024±0.012	0.032±0.010	0.105±0.035	0.038±0.014	0.165±0.019	N.D.
Na	1861±17.1	1777±69.1	1583±3.8	1542±47	2107±40	2190±60	2141±43
Mg	60.7±6.63	152±58.6	41.7±3.73	29.0±3.36	90.7±13.8	96.1±22.6	85.6±12.2
Al	127±20.9	260±107	32.6±9.12	111±22	29.4±13.3	223±70	121±26
P	83.0±6.57	103±8.7	88.3±4.25	96.7±6.21	116±11	468±129	150±26
S	363.4±34.1	402±64	346±41	396±78	348±39	475±38	478±44
K	48.6±3.8	35.4±7.47	24.45±7.19	52.5±12.8	18.0±1.21	37.9±10.8	12.4±2.43
Ca	403000±6100	378300±3300	354015±1864	354000±14000	407000±11000	400000±5900	397000±6900
Ti	21.4±1.07	50.0±17.9	11.0±0.59	12.7±0.88	14.9±2.53	15.0±4.75	14.6±2.35
Mn	337±42.8	707±56	343±51	383±12	365±44	961±93	685±75
Fe	677±107	418±131	68.7±20.6	1400±222	202±43	1630±527	655±191
Cu	10.1±0.67	2.2±0.42	3.3±0.58	4.2±0.39	4.7±0.43	5.7±0.35	9.2±0.34
Zn	20.1±2.05	13.1±0.66	13.3±2.43	20.4±1.86	17.2±1.9	6.85±1.17	7.9±0.68
Sr	1084±28	388±5.4	628±35	584±21	608±26	361±2	263±10
Y	0.046±0.024	0.085±0.04	0.03±0.00	0.257±0.024	0.027±0.001	0.276±0.114	0.019±0.013
Zr	0.338±0.044	0.328±0.102	0.097±0.016	0.242±0.034	0.107±0.032	0.835±0.133	0.593±0.028
Sb	0.17±0.03	0.13±0.02	0.107±0.007	0.127±0.009	0.10±0.04	0.031±0.007	0.033±0.008
Ba	41.9±0.86	20.6±1.55	80.5±8.24	61.0±3.48	23.5±1.77	19.5±5.37	15.5±1.53
La	0.105±0.032	0.026±0.014	0.080±0.032	0.317±0.036	0.032±0.017	0.152±0.049	0.022±0.005
Ce	0.153±0.045	0.038±0.015	0.142±0.046	0.714±0.096	0.014±0.004	0.317±0.115	0.029±0.010
Pr	0.049±0.002	0.034±0.011	0.036±0.001	0.096±0.016	0.037±0.003	0.045±0.017	0.006±0.001
Nd	0.141±0.026	0.059±0.007	0.063±0.023	0.344±0.058	0.073±0.035	0.221±0.083	0.034±0.007
Gd	0.020±0.001	0.014±0.007	0.007±0.004	0.056±0.013	0.008±0.002	0.055±0.018	0.013±0.002
Pb	0.467±0.007	0.100±0.040	0.049±0.019	3.32±0.485	0.030±0.000	0.095±0.011	0.201±0.024

Elemental composition of water and bottom sediments

The concentrations of chemical elements in water and bottom sediments are presented in Tables 3 and 4.

The highest average concentrations (n = 7) were found in water samples from the studied lakes for sodium (18100±5400 ppb), magnesium (6100±3200 ppb), silicium (6400±2200 ppb), sulfur (7000±5400

ppb), potassium (1900±460 ppb), calcium (12400±6300 ppb), boron (131±107 ppb), iron (117±40 ppb), and manganese (92±87 ppb) (Table 3). The highest average concentrations (n = 7) of the following elements were measured in bottom sediment samples: sodium (15400±2400 ppm), magnesium (13400±3900 ppm), aluminum (59400±8300 ppm), potassium (10000±2200 ppm), calcium (26800±8000 ppm), titanium (3200±520 ppm), manganese (2410±1630 ppm), iron (38500±6950 ppm), barium (337±46.4 ppm), and lead (29.0±10.3 ppm) (Table 4).

Table 3. Major and trace element composition of water (concentrations, ppb) from the studied lakes.

Element	*Chernoye Lake, Sakhalin Island*	*Peschanoye Lake, Kunashir Island*	*Bolshoye Vavayskoye Lake, Sakhalin Island*	*Vaskovskoye Lake, Primorsky Krai*	*Lebedinoye Lake, Iturup Island*	*Kurazhechnoye Lake, Kamchatka Peninsula*	*Khalaktyrskoye Lake, Kamchatka Peninsula*
Li	1.47	0.756	0.791	0.241	0.961	0.887	9.83
B	59.3	15.3	15.4	8.2	13.6	770	32.4
Na	21900	17200	7780	5170	14400	12600	47800
Mg	4130	2440	1530	619	3100	6120	24500
Al	28.5	4.9	20.1	12.5	11.7	11.7	11.9
Si	485	11017	1022	4073	14913	10723	2439
P	6.3	6.3	6.3	6.3	37.8	22.4	257
S	967	1590	1170	1260	1570	2910	39400
K	2820	1320	722	399	2070	2050	3880
Ca	4700	5330	2760	2610	5760	17300	48600
Mn	8	5.4	1.4	9.2	4.3	1.8	614
Fe	328	21.5	121	78.6	161	78	27
Zn	9.1	21.1	1.4	1.7	0.69	0.96	0.65
Sr	74.8	20.8	19.8	17	36.5	65.9	204
Zr	0.024	0.004	0.061	0.042	0.018	0.015	0.023
Ba	8.8	0.76	7.4	3.7	2.4	6.2	11.6
La	0.032	0.002	0.052	0.07	0.011	0.002	0.005
Ce	0.08	0.004	0.089	0.116	0.031	0.004	0.013
Pr	0.009	0.001	0.013	0.019	0.004	0.001	0.002
Nd	0.043	0.002	0.058	0.084	0.018	0.004	0.007
Gd	0.009	0.001	0.014	0.017	0.003	0.003	0.003
Pb	0.36	0.01	0.16	0.31	0.033	0.032	0.01

Element distribution coefficients between the shell and the environment

Apparent distribution coefficients of major and trace elements between the water and the $CaCO_3$ shells of freshwater bivalve mollusks were calculated based on several replicates from the same site. Calcium-normalized distribution coefficients $K_{d\ Shell/Water}$ = ([Element]/[Ca])$_{Shell}$/([Element]/[Ca]$_{Water}$) between shells and water samples varied from 0.00003 for K to 21.6 for Mn. The $K_{d\ Shell/Water}$ values for Mn ranged from 0.145 to 21.6, Fe from 0.002 to 15.6, Al from 0.006 to 4.53, P from 0.039 to 0.483, S from 0.001 to 0.008, Na from 0.001 to 0.0076, K from 0.0001 to 0.0022, Mg from 0.0001 to 0.0015. Calcium-normalized

distribution coefficients of trace elements between shells and bottom sediments ($K_{d\ Shell/Sediment}$ = ([Element]/[Ca])$_{Shell}$/([Element]/[Ca]$_{Sediment}$)) ranged from 0.000004 for Al to 0.23 for Sr. The values of $K_{d\ Shell/Sediment}$ for Sr ranged from 0.051 to 0.23, S from 0.0035 to 0.181, Mn from 0.0068 to 0.104, P from 0.00149 to 0.052, Zn 0.0015 to 0.03, Na from 0.0015 to 0.0141, Ba from 0.001 to 0.013, Fe from 0.000018 to 0.00651, Pb from 0.00002 to 0.00267, K from 0.000009 to 0.00128, Mg from 0.00008 to 0.00091, Al from 0.000004 to 0.000721. Distribution coefficients $K_{d\ Shell/Sediment}$ Al and $K_{d\ Shell/Water}$ Al exhibited significant relationships among samples from studied localities ($R^2 = 0.85$, $p < 0.001$). The highest values of both distribution coefficients were observed for samples from the Kamchatka Peninsula and Kunashir Island (Figure 5).

Table 4. Major and trace element composition of bottom sediments (concentrations, ppm) from the studied lakes (concentrations, ppm).

Element	*Chernoye Lake, Sakhalin Island*	*Peschanoye Lake, Kunashir Island*	*Bolshoye Vavayskoye Lake, Sakhalin Island*	*Vaskovskoye Lake, Primorsky Krai*	*Lebedinoye Lake, Iturup Island*	*Kurazhechnoye Lake, Kamchatka Peninsula*	*Khalaktyrskoye Lake, Kamchatka Peninsula*
Li	28.1	6.2	30.7	27.4	10.2	15.5	9.3
Na	8950	16300	7880	10600	19100	21400	23400
Mg	4760	25400	3520	1580	15600	16300	26700
Al	52400	49800	29100	41100	79100	76600	88000
P	969	427	238	216	361	1700	709
S	1660	228	115	172	432	3450	611
K	11600	2980	10600	20600	7690	11430	5230
Ca	8060	29300	2640	9310	44600	34700	59000
Ti	2520	4130	1500	1540	3390	4100	5080
Mn	316	2040	278	927	89	1140	12100
Fe	29800	58900	15700	16400	42700	46200	59800
Cu	70.4	6.1	9.3	10.4	17.7	79.4	55.8
Zn	230	106	36.7	164	67.8	70.6	150
Sr	268	145	86.5	80.1	308	362	357
Y	14.5	17.9	6.71	12.6	15.0	18.8	19.1
Zr	73.2	41.9	34.5	61.6	64.1	109	78.1
Sb	1.87	0.273	0.401	5.65	0.288	0.635	0.438
Ba	407	139	355	452	274	483	250
La	14.1	2.9	17.2	23.3	6.8	9.2	4.4
Ce	32.1	6.7	32.8	45.2	14	21.8	11.1
Pr	3.7	1	3.5	5	1.9	2.9	1.7
Nd	15.1	5.3	12.7	17.9	8.7	13.3	7.8
Gd	28.1	6.2	30.7	27.4	10.2	15.5	9.3
Pb	63.5	4.9	9.9	48.2	8.1	7.5	61.2

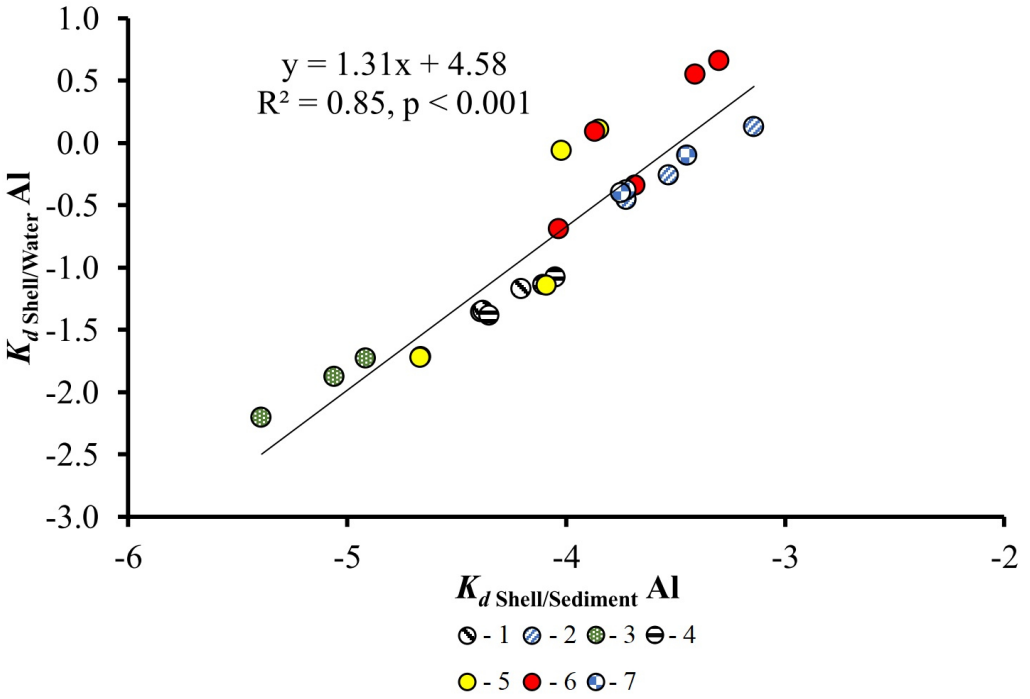

Figure 5. Relationships between K_d Shell/Sediment Al and K_d Shell/Water Al: (1) Peschanoye Lake, Kunashir Island, (2) Bolshoye Vavayskoye Lake, Sakhalin Island, (3) Vaskovskoye Lake, Primorsky Krai, (4) Lebedinoe Lake, Iturup Island, (5) Kurazhechnoye Lake, Kamchatka Peninsula, (6) Khalaktyrskoye Lake, Kamchatka Peninsula, (7) Chernoye Lake, Sakhalin Island.

Environmental factors, controlling elemental composition and shape of shells

PCA treatment of major and trace element concentrations

A preliminary assessment of the suitability of concentration data on Li, Na, Mg, Al, K, Mn, Fe, Zn, Sr, Zr, Sb, Ba и REEs in shells for factorization revealed an acceptable value of the Kaiser–Mayer–Olkin sample adequacy measure (0.639), and a statistically significant indicator of Bartlett's sphericity criterion ($\chi 2 = 466$; $p < 0.001$). We revealed three factors, capable of describing 84 % of the total variance, including Factor 1 = 38 %, Factor 2 = 36 %, and Factor 3 = 10 %. These three factors were interpreted as follows, in terms of the values of factor loadings. Factor 1 could be related to bottom sediments and accumulation of metals in shells, such as Al (0.742), Mn (0.872), Fe (0.726), Zr (0.942), and Na (0.726). Factor 2 could have a relationship with the primary productivity of freshwater ecosystems in studied waterbodies due to its high loadings for the following elements: K (0.865), Fe (0.606), Zn (624), Ba (0.609), Sr (0.539), Sb (0.561) and REE (Pr = 0.920, Nd = 0.847). Factor 3 has high loadings for Mg (0.781), Al (0.568) and Sb (0.543) and may be associated with the composition of sedimentary rocks.

Additionally, the revealed factors 1 and 2, which described 74.0 % of the total variance of studied variables, allow to divide studied samples into two groups (Mann–Whitney U test, $p < 0.01$; Figure 6). These groups correspond to the two large areas: 1) Kamchatka Peninsula; 2) Kurile Islands, Sakhalin Island, and Primorsky Krai.

Comparison of shell samples by concentration of major and trace elements

There were significant differences in elemental composition of shells between two large areas: (1) Kamchatka Peninsula; (2) Kuril Islands, Sakhalin Island, and Primorsky Krai. The concentrations of Zn, Sr, Sb, and Ba were higher in shells from waterbodies of the second region (Mann–Whitney U test, $p < 0.001$), whereas the concentrations of Na, P, Mn and Zr were higher in shells from waterbodies of the first region (Mann–Whitney U test, $p < 0.001$). Concentrations of Li, Na, P, Mn, Fe, Cu, Zn, Sr, Y, Zr, Ba, REEs, and Pb in mussels' shells exhibited significant differences among sampling localities ($p < 0.01$); concentrations of

Mg, Al, K Sb, and Nd differed between localities at $p < 0.05$ (Kruskal-Wallis H test). Only concentrations of Si, Ti, and Cr did not demonstrate significant differences between studied localities (Kruskal-Wallis H test, $p > 0.05$). Distribution coefficient $K_{d\ Shell/Water}$ had significant differences between two geographical regions for Na, Al, P, Fe, Zn, Sr, Pb (Mann–Whitney U test, $p < 0.01$). Distribution coefficients $K_{d\ Shell/Sediment}$ of Na, Al, Mn, and Fe also exhibited differences between these samples (Mann–Whitney U test, $p < 0.005$). Both distribution coefficients demonstrate higher values in samples from Kamchatka Peninsula.

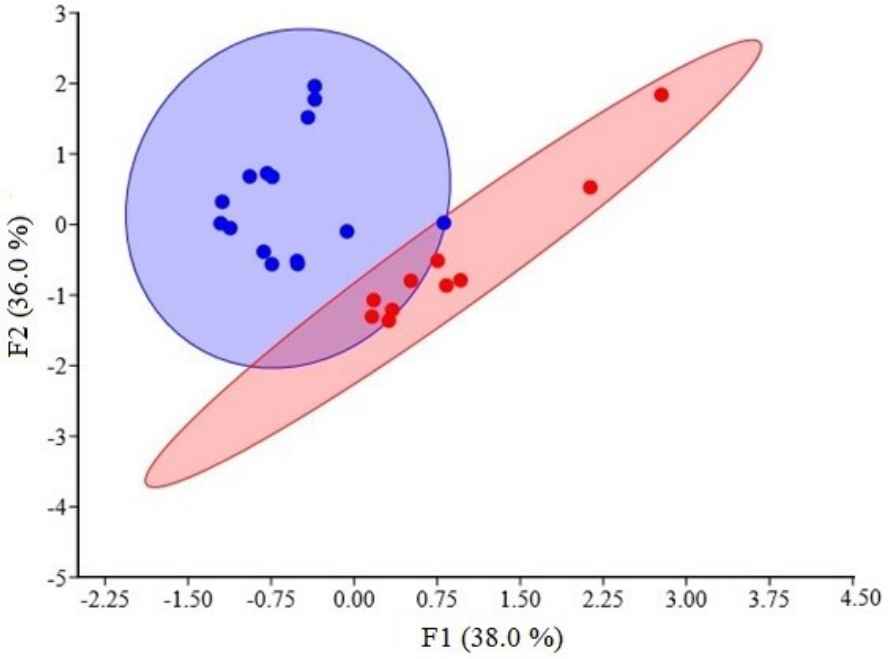

Figure 6. Normed PCA factorial graph F1 × F2 of two revealed geographical groups of *Beringiana beringiana* samples (blue circles indicate samples from Primorsky Krai, Kunashir, Sakhalin, and Iturup islands; red circles indicate samples from Kamchatka Peninsula). Ellipses show 95 % confidence interval.

Relationships between shape of valves and elemental composition of shells, water and bottom sediment.

There were significant relationships between the shell shape and Ca-normalized concentration of zinc in shells ($R^2 = 0.50$, $p < 0.001$) (Figure 7A). High concentrations of Zn were determined in shells collected from the sandy bottom; these shells had a flattened shape of the lower edge. Variation of this parameter of shell shape was higher in samples from group 2, as revealed by PCA. Coefficients of variation of Zn : Ca – ratio were 26 % for group of samples from lakes of the Kamchatka Peninsula and 29 % for samples from the Kuril Islands, Sakhalin Island, and Primorsky Krai.

Ca-normalized concentrations of Cu in shells exhibited significant relationships with the shape of shells. Their highest values among the presented samples were observed for shells from Kamchatka Peninsula (Figure 7B). Coefficients of variation of Cu : Ca – ratio were determined as 32.8 % for samples from Kamchatka Peninsula and 27.5 % for samples from the Kuril Islands, Sakhalin Island, and Primorsky Krai. We found significant regression relationships between the shape of mussels' shells and the distribution coefficients of zinc between shells and water ($R^2 = 0.52$, $p < 0.001$) (Figure 8A). There was a link between the contour of the lower edge of shells and the chemical composition of the sub-bottom water layer. Specifically, we revealed a dependence of shells' shape from the distribution coefficient $K_{d\ Shell/Water}$ Sr ($R^2 = 0.44$, $p < 0.001$) (Figure 8B). High concentrations of Sr in shells compared to water were measured for localities of the Kurile Islands, Sakhalin, and Primorsky Krai. Higher variation in values of $K_{d\ Shell/Water}$ Sr was determined for samples collected in the Kamchatka Peninsula.

The distribution coefficients of Al ($K_{d\ Shell/Water}$) and shape of the lower edge of mussels' shells also demonstrated significant relationships (Figure 8C) ($R^2 = 0.32$, $p < 0.01$). The highest values of $K_{d\ Shell/Water}$ Al were found in samples from Kamchatka Peninsula. These samples have lower variation compared to ones from Primorsky Krai, Kurile Islands, and Sakhalin Islands.

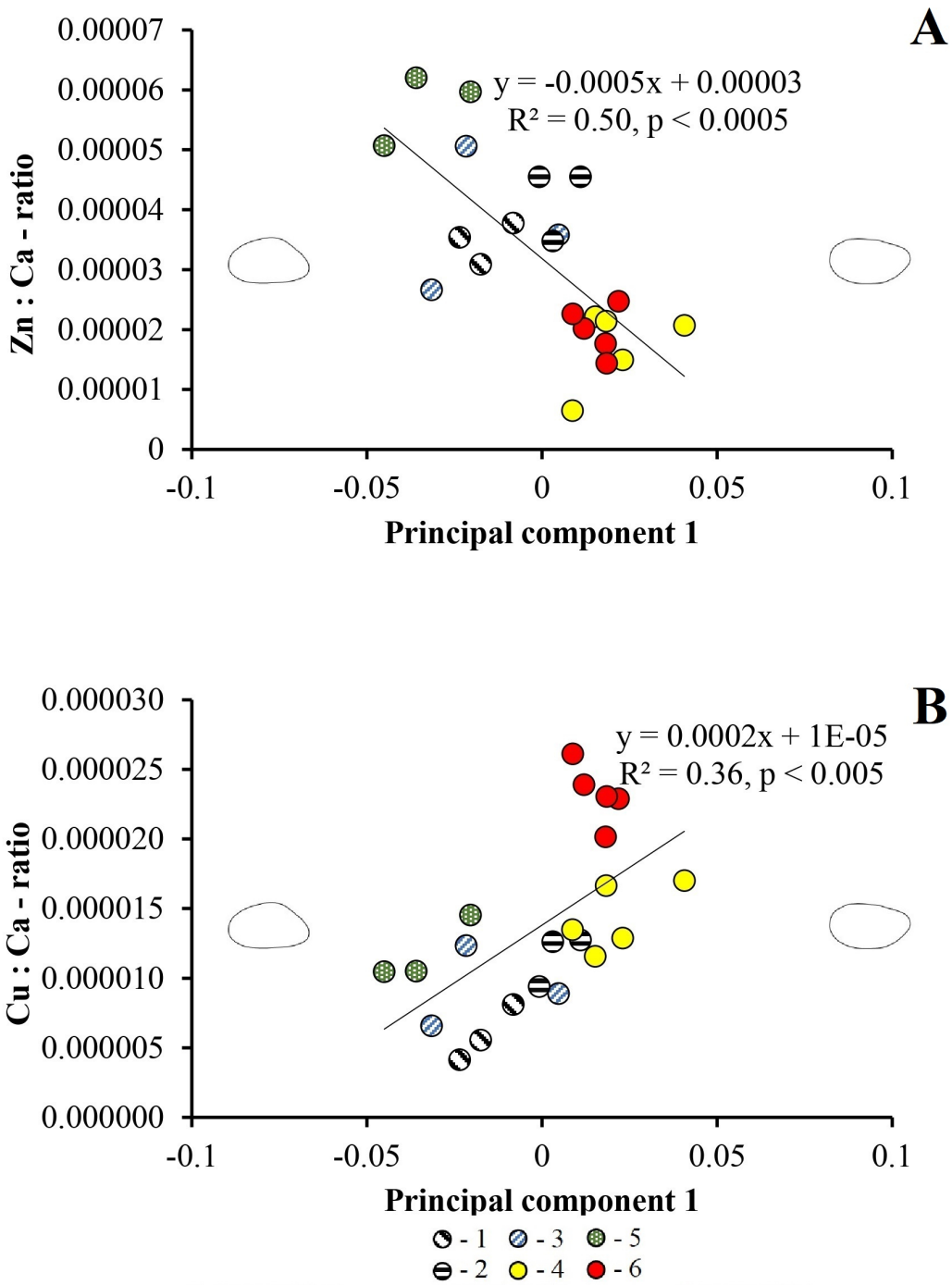

Figure 7. Relationships between Ca-normalized concentration of zinc in shells and principal component 1, (A), copper in shells and principal component 1 (B), revealed from the shell shape analysis of *Beringiana beringiana*: (1) Peschanoye Lake, Kunashir Island, (2) Lebedinoe Lake, Iturup Island, (3) Bolshoye Vavayskoye Lake, Sakhalin Island, (4) Kurazhechnoye Lake, Kamchatka Peninsula, (5) Vaskovskoye Lake, Primorsky Krai, (6) Khalaktyrskoye Lake, Kamchatka Peninsula.

We inferred the longitudinal cross-sectional area of shells from the results of Fourier analysis of the shell shape that represent the size of studied samples. This parameter of mussels' shells demonstrated relationships with several parameters of the abiotic environment. For example, Ca-normalized concentrations of zinc had significant relationships with the shell size ($R^2 = 0.59$, $p < 0.001$). The lowest Zn concentrations corresponded to the largest shells of *B. beringiana* (Figure 9).

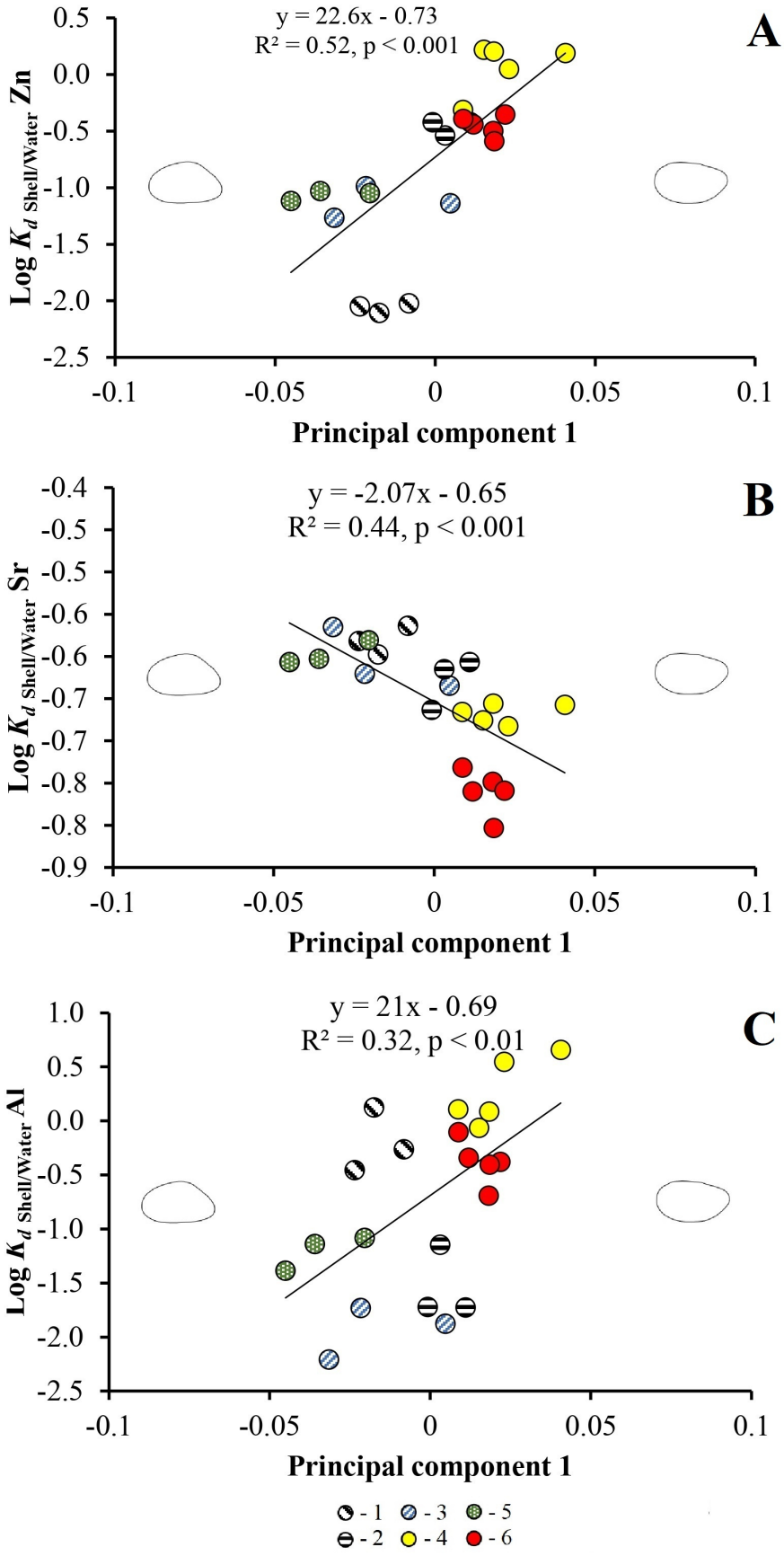

Figure 8. Relationships between values of distribution coefficients (K_d Shell/Water Zn (A), K_d Shell/Water Sr (B) and K_d Shell/Water Al (C)) and principal component 1, revealed from the shell shape analysis of *Beringiana beringiana*. For the numbers of localities see caption for Figure 7.

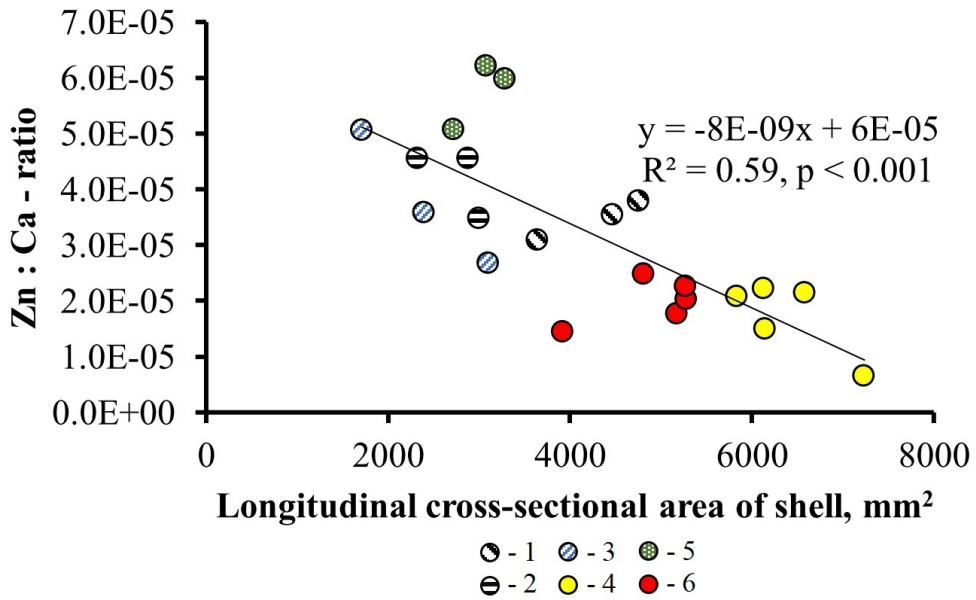

Figure 9. Relationships between Zn : Ca – ratio in *Beringiana beringiana* shells and longitudinal cross-sectional area of shell (mm^2), revealed from shell shape analysis of *Beringiana beringiana*. For the numbers of localities see caption for Figure 7.

Distribution coefficients of Al ($R^2 = 0.73$, $p < 0.001$), P ($R^2 = 0.54$, $p < 0.01$), and Fe ($R^2 = 0.78$, $p < 0.001$) between shell and water demonstrated significant relationships with the longitudinal cross-sectional area of studied shells (Figure 10). The highest values of each distribution coefficient were observed for the largest shells collected in Kamchatka Peninsula.

Additionally, a longitudinal cross-sectional area of shells demonstrated significant relationship with the distribution coefficient of Al between the shell and the sediment ($R^2 = 0.42$, $p < 0.005$). The highest values of this distribution coefficient were observed for samples from the Kunashir Island and the Kamchatka Peninsula (Figure 11).

Discussion

Mechanisms of major and trace element accumulation in B. beringiana shells

B. beringiana is a widely distributed species that was collected by us in several distant localities across large territories of freshwater basins of Northeast Asia (Figure 1). Available data on the number of COI unique haplotypes in studied populations suggest relatively low genetic diversity of *B. beringiana* (Bulakhova et al., 2023). At the same time, analysis of the shell shape demonstrated that its morphological characteristics are highly variable among localities with different environments (Figures 2, 3). The Ca-normalized concentrations of metals in the shells of mussels were distributed according to geographical locations and hydrological characteristics of lakes. For example, the highest concentrations of K, Fe, Zn, Y, REEs, and Pb were observed in Lake Vaskovskoe (Primorsky Krai); the maximum concentration of Li, Na, P, Mn, and Zr were determined in Lake Kurazhechnoye (Kamchatka Peninsula); Mg and Al reached the highest concentration in Lake Peschanoye (Kunashir Island), Sr and Sb demonstrated the maximum concentration in shells from Lake Chernoye (Sakhalin Island), Cu and Ba had the highest concentrations in the Khalaktyrskoye and Bolshoye Vavayskoye lakes, respectively (Kruskal–Wallis H test, $p < 0.05$).

Shells from Lake Vaskovskoye (Primorsky Krai) exhibited the highest concentrations of Fe and relatively high concentrations of Al, Zn and Pb. Previously, the patterns of heavy metal accumulation in the tissues of large bivalve mollusks were described based on samples of *B. beringiana* from this lake (Lysenko & Chernova, 2014). Our results on the concentrations of Fe, Mn, Cu, An, and Pb in the bottom sediments of Lake Vaskovskoe are consistent with those of Chernova et al. (2014a). The concentration of these elements in the sediments of Lake Vaskovskoe obtained in this study fall into the range of values for sandy and aleuropelite (silty clay) fraction reported by Chernova et al. (2014a).

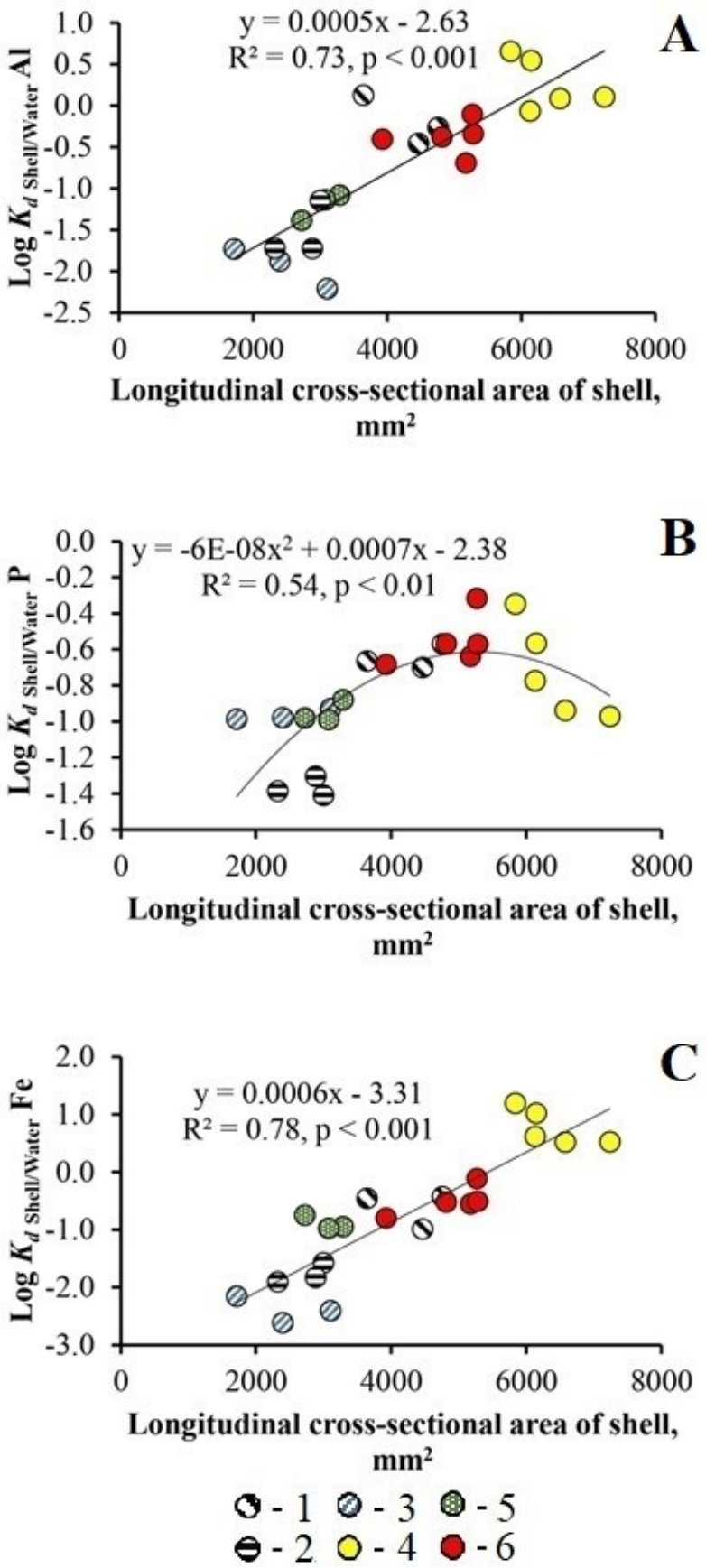

Figure 10. Relationships between values of $K_{d\ \text{Shell/Water}}$ Al (A), $K_{d\ \text{Shell/Water}}$ P (B), $K_{d\ \text{Shell/Water}}$ Fe (C) and longitudinal cross-sectional area of shell (mm^2), revealed from the shell shape analysis of *Beringiana beringiana*. For the numbers of localities see caption for Figure 7.

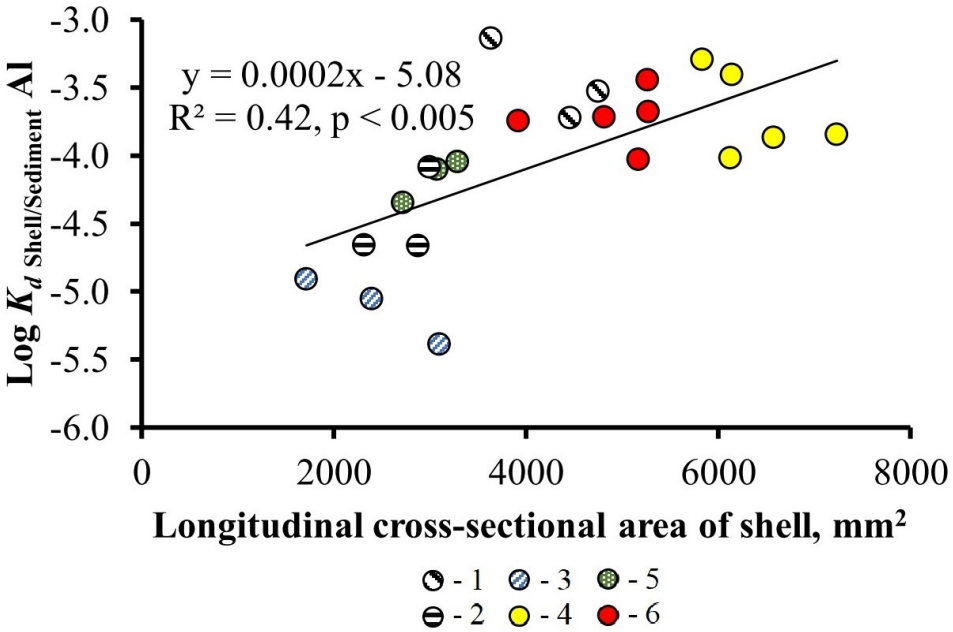

Figure 11. Relationships between values of $K_{d\ \text{Shell/Sediment}}$ Al and longitudinal cross-sectional area of shell (mm^2), revealed from the shell shape analysis of *Beringiana beringiana*. For the numbers of localities see caption for Figure 7.

The Chernoye Lake is located in an area that is polluted by outdoor airborne particles (fly ash) from the coal-fueled power plants of Uglegorsk town (the nearest of them is located in 1 km from the lake) (Report …, 2023). These local anthropogenic emissions could lead to contamination of freshwater habitats by heavy metals (Tiwari et al., 2008). Consistent with this possibility, shells of the Beringian mussels from the Chernoye Lake exhibited the highest concentrations of antimony (Kruskal-Wallis test H, $p < 0.05$) and strontium (Kruskal-Wallis test H, $p < 0.005$). It should be noted that the density of studied mussels in the lake is relatively high despite the contamination by pollutants.

PCA analysis of Ca-normalized concentrations

Differences in environments of the habitats were assessed by multivariate analysis of Ca-normalized concentrations. According to the results of factor analysis, the first factor reflected the relationship between the elemental composition of shells and the composition of bottom sediments in lakes. This factor was positively related to Al, Fe and Mn concentrations in shells. Several authors (Langlet et al., 2007; Zhao et al., 2017) noted that in anoxic environments of silted bottom, redox-sensitive elements are present in bioavailable form (Mn^{2+}, Fe^{2+}). Accordingly, we believe that the first factor shows that under the conditions described above, mollusks accumulate iron and manganese in their shells from the bottom sediments. Consequently, the distribution coefficient of Mn between the shell and bottom sediments had the highest values (Kruskal–Wallis H test, $p < 0.001$) in localities with a clay bottom (Lake Khalaktyrskoye and Lake Kurazhechnoye). At the same time, the distribution coefficient of manganese between shell and water does not follow this pattern.

Factor 2 may be related to the primary productivity, i.e. to the organic matter consumed by mussels, accompanied by element uptake via both active (bioavailable ions and low molecular weight organic complexes) and passive (metal oxy(hydr)oxides) forms. The latter may include the trace element uptake from mineral and organic suspended matter, including phytoplankton. It is known that the mussels, being filtrators, consume not only dissolved forms of elements (< 0.45 micron) but also the suspended material such as phytoplankton, organic detritus, and silicate particles (Alber & Valiela, 1994; Gagnon & Fisher, 1997; Jaeschke et al., 2015). A relationship of factor 2 with the uptake of organic matter may be established based on high factor loadings for potassium (0.865) and barium (0.609). Jaworski et al. (2003) reported that potassium may have limited influence on the mass of phytoplankton in a water body, which is one of the nutrients for freshwater mussels. The concentration of barium in the shells of mussels may correlate with the phytoplankton bloom directly (Hatch et al., 2013; Marali et al., 2017), and it may be also related to the level of organic matter in waterbody. Additionally, the highest values of this factor were observed in the lakes,

located in the southern part of the studied territory (incl. Vaskovskoe Lake and lakes of Sakhalin Island), where the phytoplankton blooms are more likely to occur.

Factor 3 had high loadings for Mg (0.781), Al (0.568) and Sb (0.543) and may be associated with the composition of sedimentary rocks (Greenwood & Earnshaw, 1997) or the hydrothermal groundwater input as it is known from geochemical studies of rivers in the Kamchatka Peninsula (Dessert et al., 2009). For example, antimony oxide is a component of the weathering products of rocks, and concentrations of magnesium may reflect high ratio of volcanic to sedimentary rocks, observed within active geothermal provinces.

Significant variance in values of Factor 1 and Factor 2 was observed within the group that included samples from the freshwater basins of Primorsky Krai, Sakhalin Island, and the Kurile Islands. Inside this group, samples have clear division by localities, therefore corroborating previously described geographical (site/landscape-induced) control on trace element accumulation pattern in the shells of freshwater bivalves (Bolotov et al., 2015; Lyubas et al., 2021; Lyubas et al., 2023).

Variability of the shell shape in Beringian mussel populations

The shape of *B. beringiana* shells is known to reflect environmental parameters of the waterbody (Bulakhova et al., 2023). Here, we found that contour of the lower edge of shell varies depending on chemical composition of the bottom water layer and the type of bottom substrate. For example, Ca-normalized concentration of Cu, distribution coefficients $K_{d\ \mathrm{Shell/Water}}$ Zn, and $K_{d\ \mathrm{Shell/Water}}$ Al had positive relationships with the form of shell's lower edge.

Among the unionid mussels, the positive relationship between the habitat conditions and shell morphology is known for the genera *Unio* and *Anodonta*. In particular, there is a correspondence between the contour shape and the type of habitat (stagnant vs. flowing water), as established by Zieritz & Aldridge (2011). Tomilova (2021) demonstrated that the shell shape of a widely distributed unionid mussel, *Anodonta anatina*, is dependent on the temperature in a certain geographic region, which allowed to explain large phenotypic plasticity of the shell form of this species. The analyzed species (*B. beringiana)* is also distributed across several climate zones and exhibit large variability of the shell shape (Bolotov et al., 2020). Therefore, such phenotypic plasticity may be related to environmental conditions of the habitat.

The variable "longitudinal cross-sectional area of shell", inferred from Fourier analysis, is related to concentration of zinc in shell and is also related to habitat parameters. Observed $K_{d\ \mathrm{Shell/Water}}$ of Al, P, and Fe have relationship with size and, therefore, reflect the age of individuals. It may be explained by a distribution of different-age specimens at various depths and within different substrates (Tomilova, 2021).

Conclusion

The present study confirmed the low genetic diversity of the Beringian freshwater mussel revealed in a previous study (Bulakhova et al., 2023). In Northeast Asia, only six unique haplotypes were found among 24 COI sequences. It presents a relatively small number compared to other species of the family Unionidae. At the same time, we found the high level of morphological variability of shells. The plasticity of shell shape was associated with the varied habitat environments. The concentration of chemical elements in *B. beringiana* shells was studied across contrasting physiographic regions. The highest concentrations of lithophilic elements (including Mn, Li and Zr) were found in the shells from Lake Kurazhechnoye (Kamchatka Peninsula). The highest concentrations of Al and Mg were found in shells from Lake Peschanoye (Kunashir Island). In Lake Chernoye (Sakhalin Island) were detected the highest concentrations of Sr and Sb in shells. Zn, Fe, Pb, and rare earth elements were present in large concentrations in shells from Lake Vaskovskoye in Primorsky Krai.

Overall, new data on the concentration of major and trace elements in the shells of a widespread freshwater bivalve species and associated environmental components (water and bottom sediments) allow to evaluate the factors related to the variability of shell shape, as well as to reconstruct the environments of specific habitats of freshwater mussels in surface waters.

Acknowledgements

This research was funded by the Russian Science Foundation (Grant Number 21-17-00126 to I.N.B., A.A.L., T.A.E., I.V.V., E.S.K., M.Y.G. and I.S.K. (including fieldworks in Kamchatka Peninsula and Primorsky Krai, preparation of samples, molecular and chemical analyses, statistical treatment of data). Fieldwork in the Sakhalin Region was carried out with the financial support of the Russian Science Foundation (project No. 21-74-10155 to O.V.A., A.V.Kr. and A.S.A.). O.S.P. was partially supported by the TSU Development Program "Priority-2030" (including preparation of the manuscript).

References

Alber, M. & Valiela, I. (1994) Incorporation of organic aggregates by marine mussels. *Marine Biology,* 121, 259–265.

Bandelt, H.J., Forster, P. & Röhl, A. (1999) Median-joining networks for inferring intraspecific phylogenies. *Molecular Biology and Evolution,* 16, 37–48.

Bogatov, V.V., Prozorova, L.A., Chernova, E.N., Lysenko, E.V., Ngo, X., Tran, T. & Hoang, N. (2019) Bioaccumulation of Heavy Metals in Soft Tissues of Bivalve Mollusks from Natural Lakes in Eastern Sikhote-Alin (Russia) and the Mekong Delta (Vietnam). *Doklady Earth Sciences*, 484, 2, 206–208.

Bogatov, V.V. & Bogatova, L.V. (2009) Heavy metal accumulation by freshwater hydrobionts in a mining area in the south of the Russian Far East. *Russian Journal of Ecology*, 40 (3), 187–193.

Bolotov, I.N., Pokrovsky, O.S., Auda, Y., Bespalaya, J.V., Vikhrev, L.V., Gofarov, M.Y., Lyubas, A.A., Viers, J. & Zouiten, C. (2015) Trace element composition of freshwater pearl mussels *Margaritifera* spp. across Eurasia: Testing the effect of species and geographic location. *Chemical Geology*, 402, 125–139. https://doi.org/10.1016/j.chemgeo.2015.03.006

Bolotov, I. N., Kondakov, A.V., Konopleva, E.S., Vikhrev, I.V., Aksenova, O.V., Aksenov, A.S., Bespalaya, Y.V., Borovskoy, A.V., Danilov, P.P., Dvoryankin, G.A., Gofarov, M.Y., Kabakov, M.B., Klishko, O.K., Kolosova, Y.S., Lyubas, A.A., Novoselov, A.P., Palatov, D.M., Savvinov, G.N., Solomonov, N.M., Spitsyn, V.M., Sokolova, S.E., Tomilova, A.A., Froufe, E., Bogan, A.E., Lopes-Lima, M., Makhrov, A.A. & Vinarski, M.V. (2020) Integrative taxonomy, biogeography and conservation of freshwater mussels (Unionidae) in Russia. *Scientific Reports*, 10, 3072, 1–20. https://doi.org/10.1038/s41598-020-59867-7

Bulakhova, N.A., Makhrov, A.A., Lazutkin, A.N., Shekhovtsov, S.V., Poluboyarova, T.V. & Berman, D.I. (2023) Beringian freshwater mussel *Beringiana beringiana* (Unionidae) in Northeast Asia. *Water*, 15(20), 3538. https://doi.org/10.3390/w15203538

Chernova, E.N., Lobas, L.A., Kovalev, M.Yu. & Lysenko, E.V. (2014a) Heavy metal distributions in components of aquatic ecosystems in natural monuments—Lakes Blagodati, Vas'kovskoe (Primorskii Krai) and Azabach'e (Kamchatskii Krai). *Water Resources*, 41(3), 319–324.

Chernova E.N., Shulkin V.M., Lysenko E.V., Lutsenko T.N. & Boldeskul A.G. (2014b) Hydrochemical and biogeochemical features of freshwater and brackish lakes in eastern Sikhote-Alin. *Izvestiya TINRO*, 178, 157–172.

Dessert, C., Gaillardet, J., Dupre, B., Schott, J. & Pokrovsky, O.S. (2009) Fluxes of high- versus low-temperature water-rock interactions in aerial volcanic areas: the example of the Kamchatka Peninsula, Russia. *Geochimica et Cosmochimica Acta*, 73, 148–169.

Folmer, O., Black, M., Hoeh, W., Lutz, R. & Vrijenhoek, R. (1994) DNA primers for amplification of mitochondrial cytochrome c oxidase subunit I from diverse metazoan invertebrates. *Molecular Marine Biology and Biotechnology*, 3, 294–299.

Gagnon, C. & Fisher, N.S. (1997) The bioavailability of sediment-bound Cd, Co, and Ag to the mussel *Mytilus edulis*. *Canadian Journal of Fisheries and Aquatic Sciences*, 54, 147–156. https://doi.org/10.1139/f96-256

Golovaneva, A.E. (2016) Assessment of the ecological state of lake Khalaktyrskoye by hydrochemical indicators. *Water management of Russia*, 2, 32–44.

Greenwood, N.N. & Earnshaw, A. (1997). Chemistry of the Elements, Second Edition. Butterworth-Heinemann, United Kingdom, 1341 pp. https://doi.org/10.1016/C2009-0-30414-6

Gustafson, R.G., & Iwamoto, E.M. (2005) A DNA-based identification key to pacific northwest mussel glochidia: importance to salmonid and mussel conservation. *Northwest Science*, 79(4), 233.

Hammer, O., Harper, D.A.T. & Ryan, P.D. (2001) PAST: paleontological statistics software package for education and data analysis. *Palaeontologia Electronica*, 4, 1–9.

Hatch, M.B.A., Schellenberg, S.A. & Carter, M.L. (2013) Ba/Ca variations in the modern intertidal bean clam *Donax gouldii*: An upwelling proxy? *Palaeogeography, Palaeoclimatology, Palaeoecology*, 373, 98–107. https://doi.org/10.1016/j.palaeo.2012.03.006

Iwata, H. & Ukai, Y. (2002) SHAPE: a computer program package for quantitative evaluation of biological shapes based on elliptic fourier descriptors. *The Journal of Heredity*, 93, 384–385. https://doi.org/10.1093/jhered/93.5.384

Jaeschke, B.C., Lind, O.C., Bradshaw, C. & Salbu, B. (2015) Retention of radioactive particles and associated effects in the filter-feeding marine mollusc *Mytilus edulis*. *Science of The Total Environment*, 502, 1–7. https://doi.org/10.1016/j.scitotenv.2014.09.007

Jaworski, G.H.M., Talling, J.F. & Heaney, S.I., (2003) Potassium dependence and phytoplankton ecology: an experimental study. *Freshwater Biology*, 48, 833–840. https://doi.org/10.1046/j.1365-2427.2003.01051.x

Johnson, M., Zaretskaya, I., Raytselis, Y., Merezhuk, Y., McGinnis, S., & Madden, T.L. (2008) NCBI BLAST: a better web interface. *Nucleic Acids Research*, 36, W5–W9. https://doi.org/10.1093/nar/gkn201

Karandashev, V.K., Turanov, A.N., Orlova, T.A., Lezhnev A.E., Nosenko S.V., Zolotareva N.I., & Moskvina, I.R. (2008) Use of the inductively coupled plasma mass spectrometry for element analysis of environmental objects. *Inorganic Materials,* 44, 1491–1500. https://doi.org/10.1134/S0020168508140045

Klishko, O.K., Berdnikov, N.V., Bogan, A.E. & Vinarski, M.V. (2022) Shells of Pearlmussels, *Margaritifera dahurica* (Bivalvia: Margaritiferidae), as a biogeochemical indicator of the background (Holocene) and current major and trace elements content in riverine waters of Transbaikalia (southeast Siberia). *Ecological Indicators*, 134, 108482. https://doi.org/10.1016/j.ecolind.2021.108482

Langlet, D., Alleman, L.Y., Plisnier, P.D., Hughes, H. & Andre, L. (2007) Manganese content records seasonal upwelling in Lake Tanganyika mussels. *Biogeosciences,* 4, 195–203. https://doi.org/10.5194/bg-4-195-2007

Lopes-Lima, M., Hattori, A., Kondo, T., Lee, J.H., Kim, S.K., Shirai, A., Hayashi, H., Usui, T., Sakuma, K., Toriya, T., Sunamura, Y., Ishikawa, H., Hoshino, N., Kusano, Y., Kumaki, H., Utsugi, Y., Yabe, S., Yoshinari, Y., Hiruma, H., Tanaka, A., Sao, K., Ueda, T., Sano, I., Miyazaki, J.-I., Gonçalves, D.V., Klishko, O.K., Konopleva, E.S., Vikhrev, I.V., Kondakov, A.V., Gofarov, M.Yu., Bolotov, I.N., Sayenko, E.M., Soroka, M., Zieritz, A., Bogan, A.E. & Froufe, E. (2020) Freshwater mussels (Bivalvia: Unionidae) from the Rising Sun (Far East Asia): Phylogeny, systematics, and distribution. *Molecular Phylogenetics and Evolution*, 146, 1–27. https://doi.org/10.1016/j.ympev.2020.106755

Lysenko, E.V. & Chernova, E.N. (2014) Bioaccumulation of microelements in the trophic chain "water – plankton – filter-feeding mollusks" in lakes of northeastern Sikhote-Alin with different levels of anthropogenic load // *Biogeochemistry of chemical elements and compounds in natural environments: Materials of the International School-Seminar for Young Researchers, Tyumen, May 13-16, 2014. Tyumen: Tyumen State University Publishing House*, 215–220.

Lyubas, A.A., Kuznetsova, I.A., Bovykina, G.V., Eliseeva, T.A., Gofarov, M.Y., Khrebtova, I.S., Kondakov, A.V., Malkov, A.V., Mavromatis, V., Shevchenko, A.R., Soboleva, A.A., Pokrovsky, O.S. & Bolotov, I.N. (2023) Trace element patterns in shells of mussels (Bivalvia) allow to distinguish between fresh- and brackish-water coastal environments of the subarctic and boreal zone. *Water*, 15(20), 3625. https://doi.org/10.3390/w15203625

Lyubas, A.A., Tomilova, A.A., Chupakov, A.V., Vikhrev, I.V., Travina, O.V., Orlov, A.S., Zubrii, N.A., Kondakov, A.V., Bolotov, I.N. & Pokrovsky, O.S. (2021) Iron, phosphorus and trace elements in mussels' shells, water, and bottom sediments from the Severnaya Dvina and the Onega River basins (Northwestern Russia). *Water*, 13, 3227. https://doi.org/10.3390/w13223227

Marali, S., Schöne, B.R., Mertz-Kraus, R., Griffin, S.M., Wanamaker, A.D., Matras, U. & Butler, P.G. (2017) Ba/Ca ratios in shells of *Arctica islandica* – potential environmental proxy and crossdating tool. *Palaeogeography, Palaeoclimatology, Palaeoecology*, 465, 347–361. https://doi.org/10.1016/j.palaeo.2015.12.018

Report on the state and protection of the environment of the Sakhalin region in 2022. (2023) Ministry of Ecology and Development of the Sakhalin region Yuzhno-Sakhalinsk, Akon LLC. 190 pp.

Thompson, J.D., Higgins, D.G. & Gibson, T.J. (1994) CLUSTAL W: improving the sensitivity of progressive multiple sequence alignment through sequence weighting, position-specific gap penalties and weight matrix choice. *Nucleic acids research*, 22 (22), 4673–4680. https://doi.org/10.1093/nar/22.22.4673

Tiwari, S., Kumari, B. & Singh, S. (2008) Evaluation of metal mobility/immobility in fly ash induced by bacterial strains isolated from the rhizospheric zone of *Typha latifolia* growing on fly ash dumps. *Bioresource Technology*, 99, 1305–1310. https://doi.org/10.1016/j.biortech.2007.02.010

Tomilova, A.A. (2021) *Morphological variability and phylogeography of the duck mussel Anodonta anatina in Russia and adjacent territories.* PhD Thesis, Papanin Institute for Biology of Inland Waters, Russian Academy of Sciences, Borok, Russia, 146 pp.

Tomilova, A.A., Kondakov, A., & Kisil, O. Y. (2019). Usage of transcribed spacers ITS1 and ITS2 for identification of freshwater mussels of the genera *Anodonta* and *Pseudanodonta* (Bivalvia: Unionidae: Anodontinae). *Zhurnal Obshchei Biologii*, 80(5), 364–371. https://doi.org/10.1134/S0044459619050075

Zhao, L., Walliser, E.O., Mertz-Kraus, R. & Schöne, B.R. (2017) Unionid shells (*Hyriopsis cumingii*) record manganese cycling at the sediment–water interface in a shallow eutrophic lake in China (Lake Taihu). *Palaeogeography, Palaeoclimatology, Palaeoecology*, 484, 97–108. https://doi.org/10.1016/j.palaeo.2017.03.010

Zieritz A. & Aldridge D.C. (2011) Sexual, habitat-constrained and parasite-induced dimorphism in the shell of a freshwater mussel (*Anodonta anatina*, Unionidae). *Journal of Morphology*, 272(11), 1365–1375. https://doi.org/10.1002/jmor.10990

Appendix 1.

List of *Beringiana beringiana COI* sequences used in this study.

Locality	Sample ID	COI sequence	References
Russia: Kamchatka Krai, Avacha River	RMBH biv169	MK034152	Tomilova et al. (2019)
Russia: Kunashir Island, Aliger Lake	RMBH biv186/2	MK574206	Bolotov et al. (2020)
Russia: Kunashir Island, Aliger Lake	RMBH biv186/4	MK574207	Bolotov et al. (2020)
Russia: Primorsky Krai, Avakumovka River	RMBH biv272/6	MK574208	Bolotov et al. (2020)
Russia: Primorsky Krai, Avakumovka River	RMBH biv272/9	MK574209	Bolotov et al. (2020)
Russia: Primorsky Krai, Vaskovskoe Lake	RMBH biv273/2	MK574210	Bolotov et al. (2020)
Russia: Primorsky Krai, Vaskovskoe Lake	RMBH biv273/8	MK574211	Bolotov et al. (2020)
Russia: Primorsky Krai, Japanese Lake	RMBH biv274/3	MK574212	Bolotov et al. (2020)
Russia: Primorsky Krai, Japanese Lake	RMBH biv274/6	MK574213	Bolotov et al. (2020)
USA: Alaska, Anchorage	RMBH biv283/1	MK574218	Bolotov et al. (2020)
USA: Alaska, Anchorage	RMBH biv283/11	MK574219	Bolotov et al. (2020)
USA: Alaska, Anchorage	RMBH biv283/12	MK574220	Bolotov et al. (2020)
USA: Alaska, Eugumen Lake	RMBH biv284/2	MK574221	Bolotov et al. (2020)
USA: Alaska, Eugumen Lake	RMBH biv284/3	MK574222	Bolotov et al. (2020)
USA: Alaska, Eugumen Lake	RMBH biv284/7	MK574223	Bolotov et al. (2020)
USA: Alaska, Birch Lake	RMBH biv286/1	MK574224	Bolotov et al. (2020)
USA: Alaska, Birch Lake	RMBH biv286/2	MK574225	Bolotov et al. (2020)
USA: Alaska, Birch Lake	RMBH biv286/4	MK574226	Bolotov et al. (2020)
Russia: Yakutia Republic, Usun-Ehbeh Lake	RMBH biv302/1	MK574214	Bolotov et al. (2020)
Russia: Yakutia Republic, Usun-Ehbeh Lake	RMBH biv302/10	MK574215	Bolotov et al. (2020)
Russia: Yakutia Republic, Usun-Ehbeh Lake	RMBH biv302/11	MK574216	Bolotov et al. (2020)
USA: Alaska, JoJo Lake	215JoJoLake	DQ272370	Gustafson & Iwamoto (2005)
Japan, Kushiro River	MHS BBHK-01	MT020555	Lopes-Lima et al. (2020)
USA: Alaska, Mud Lake	CIIMAR BIV1925	MT020556	Lopes-Lima et al. (2020)
Japan, Takkobu Lake	CIIMAR BIV2700	MT020557	Lopes-Lima et al. (2020)
USA: Alaska, Cheney Lake	CIIMAR BIV0374	MT020558	Lopes-Lima et al. (2020)
Russia: Primorsky Krai, Vaskovskoe Lake	RMBH biv1181/1	OR858608	This study
Russia: Primorsky Krai, Vaskovskoe Lake	RMBH biv1181/2	OR858609	This study
Russia: Primorsky Krai, Vaskovskoe Lake	RMBH biv1181/3	OR858610	This study
Russia: Kamchatka Krai, Kurazhechnoe Lake	RMBH biv1212/2	OR858611	This study
Russia: Kamchatka Krai, Kurazhechnoe Lake	RMBH biv1212/3	OR858612	This study
Russia: Kamchatka Krai, Kurazhechnoe Lake	RMBH biv1212/4	OR858613	This study
Russia: Kamchatka Krai, Kurazhechnoe Lake	RMBH biv1212/6	OR858614	This study
Russia: Kamchatka Krai, Kurazhechnoe Lake	RMBH biv1212/8	OR858615	This study
Russia: Kamchatka Krai, Khalaktyrskoye Lake	RMBH biv1213/2	OR858616	This study
Russia: Kamchatka Krai, Khalaktyrskoye Lake	RMBH biv1213/3	OR858617	This study
Russia: Kamchatka Krai, Khalaktyrskoye Lake	RMBH biv1213/5	OR858618	This study
Russia: Kamchatka Krai, Khalaktyrskoye Lake	RMBH biv1213/6	OR858619	This study
Russia: Sakhalin Island, Chernoe Lake	RMBH biv1248/1	OR858620	This study
Russia: Sakhalin Island, Chernoe Lake	RMBH biv1248/2	OR858621	This study

..continued on the next page

Locality	Sample ID	COI sequence	References
Russia: Sakhalin Island, Chernoe Lake	RMBH biv1248/3	OR858622	This study
Russia: Sakhalin Island, Bolshoe Vavaiskoe Lake	RMBH biv1250/1	OR858623	This study
Russia: Sakhalin Island, Bolshoe Vavaiskoe Lake	RMBH biv1250/2	OR858624	This study
Russia: Sakhalin Island, Bolshoe Vavaiskoe Lake	RMBH biv1250/3	OR858625	This study
Russia: Kunashir Island, Peschanoe Lake	RMBH biv1251/1	OR858626	This study
Russia: Kunashir Island, Peschanoe Lake	RMBH biv1251/2	OR858627	This study
Russia: Kunashir Island, Peschanoe Lake	RMBH biv1251/3	OR858628	This study
Russia: Iturup Island, Lebedinoe Lake	RMBH biv1254/1	OR858629	This study
Russia: Iturup Island, Lebedinoe Lake	RMBH biv1254/2	OR858630	This study
Russia: Iturup Island, Lebedinoe Lake	RMBH biv1254/3	OR858631	This study